ACS Chemical Neuroscience

Research Article

pubs.acs.org/chemneuro

On-Surface Aggregation of α-Synuclein at Nanomolar Concentrations Results in Two Distinct Growth Mechanisms

Michael Rabe,[†] Alice Soragni,[‡] Nicholas P. Reynolds,[†] Dorinel Verdes,[†] Ennio Liverani,[‡] Roland Riek,[‡,*] and Stefan Seeger[†,*]

[†]Institute of Physical Chemistry, University of Zurich, Winterthurerstrasse 190, 8057 Zurich, Switzerland

[‡]Laboratory of Physical Chemistry, ETH Zurich, Wolfgang-Pauli Strasse 10, 8093 Zurich, Switzerland

Supporting Information

ABSTRACT: The aggregation of α-synuclein (α-Syn) is believed to be one of the key steps driving the pathology of Parkinson's disease and related neurodegenerative disorders. One of the present hypotheses is that the onset of such pathologies is related to the rise of α-Syn levels above a critical concentration at which toxic oligomers or mature fibrils are formed. In the present study, we find that α-Syn aggregation *in vitro* is a spontaneous process arising at bulk concentrations as low as 1 nM and below in the presence of both hydrophilic glass surfaces and cell membrane mimicking supported lipid bilayers (SLBs). Using three-dimensional supercritical angle fluorescence (3D-SAF) microscopy, we observed the process of α-Syn aggregation *in situ*. As soon as α-Syn monomers were exposed to the surface, they started to adsorb and aggregate along the surface plane without a prior lag phase. However, at a later stage of the aggregation process, a second type of aggregate was observed. In contrast to the first type, these aggregates showed an extended structure being tethered with one end to the surface and being mobile at the other end, which protruded into the solution. While both types of α-Syn aggregates were found to contain amyloid structures, their growing mechanisms turned out to be significantly different. Given the clear evidence that surface-induced α-Syn aggregation *in vitro* can be triggered at bulk concentrations far below physiological concentrations, the concept of a critical concentration initiating aggregation *in vivo* needs to be reconsidered.

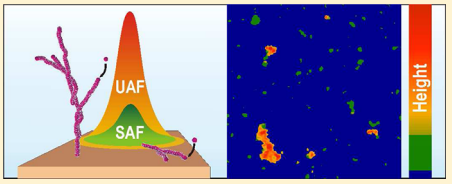

KEYWORDS: *Parkinson's disease, α-synuclein, amyloid, protein aggregates, 3D-SAF-microscopy, FRET*

α-Synuclein (α-Syn) is a small (~14.5 kDa) protein and its hypothesized function is related to vesicle trafficking and release.[1] It is predominantly expressed in neuronal presynaptic terminals in the brain, being one of the most abundant proteins with an estimated intracellular concentration of 30−60 μM.[2] α-Syn is able to self-polymerize into amyloid fibrils, and the presence of such aggregates in the form of Lewy bodies (LBs) is a characteristic pathological feature of Parkinson's disease (PD) and similar neurodegenerative disorders.[3−5] Aggregates produced from recombinant α-Syn *in vitro* are indistinguishable from those extracted from Lewy bodies of PD patients.[6,7] While most cases of PD are of the late-onset sporadic type, there are rare cases of inherited early onset PD caused by α-Syn gene triplications[8] or by the presence of point mutations that are reported to increase the oligomerization and fibrillation propensities of α-Syn.[9−11] Several *in vitro* studies have shown that the process of α-Syn aggregation in solution is concentration dependent and typically requires bulk protein concentrations above 100 μM.[12−14] From these observations derives the concept of a "critical concentration", which implies that the aggregation of amyloidogenic proteins is prevented below a minimum cytoplasmic concentration.[15−18] In line with this concept, it has been proposed that changes in α-Syn homeostasis upon aging result in an apparent increase of the cellular α-Syn concentration. This may include, for instance, alterations in the molecular crowding state due to cell shrinkage[2,19] or a breakdown of the α-Syn degradation mechanism.[20,21]

Recent studies highlighted the enhanced aggregation propensity of α-Syn in the presence of interfaces such as lipid bilayers[22,23] or suggest a surface-assisted nucleation mechanism.[24] Indeed α-Syn oligomerization and aggregation in the presence of lipid vesicles or supported lipid bilayers (SLBs) has been described at significantly lower protein bulk concentrations, in the low micromolar range.[25,26] Generally, the interaction of α-Syn with hydrophilic interfaces requires negative surface charges whereas protein adsorption is shown to be severely reduced when SLBs with zero net charge are used, implying a strong contribution of electrostatic forces during the adsorption event.[26−29] Also physiologically less relevant hydrophobic interfaces including the air−water interface were shown to accelerate fibril formation processes.[30]

Detailed information about the mechanisms and driving forces triggering protein aggregation and amyloid fiber formation is to a large extent missing.[31−33] Most accepted is a nucleation-dependent aggregation mechanism in which a slow nucleation process during which a stable seed is formed is

Received: August 21, 2012
Accepted: December 28, 2012
Published: December 28, 2012

followed by a fast protein aggregation phase.[34] In most *in vitro* experiments, which are based on probing amyloid formation in the bulk using ThT staining, the nucleation period is recognized as a lag phase in which few or no amyloid fibrils are detected.[35] This lag phase seems to be extremely sensitive to the applied experimental conditions and therefore often appears to be irreproducible. Only recently, it has been shown that the lag time is actually highly predictable if studies are performed with high experimental care.[36]

In order to get detailed insights into α-Syn aggregation on surfaces at nanomolar protein concentrations, we took advantage of the three-dimensional supercritical angle fluorescence (3D-SAF) microscopy technique, which allows highly sensitive and surface selective detection of fluorescently labeled biomolecules.[37,38] In combination with Förster resonance energy transfer (FRET) imaging, this noninvasive technique visualizes the aggregation state and the height distribution of surface bound protein assemblies *in situ*, which is the primary advantage over traditional methods such as atomic force or electron microscopy.[39] With this experimental set up, we provide evidence that α-Syn aggregation is a spontaneous surface-induced process occurring at bulk concentrations as low as 1 nM and below on negatively charged SLBs as well as on negatively charged cleaned glass surfaces.

RESULTS AND DISCUSSION

α-Syn Aggregates at Nanomolar Concentrations. The adsorption and aggregation behavior of α-Syn was monitored using the supercritical angle fluorescence (SAF) detection channel of the 3D-SAF microscope combined with FRET measurements. Donor and acceptor scan images were recorded while applying an equal mixture of donor (DY-647) and acceptor (Cy7) labeled α-Syn to a supported lipid bilayer (SLB) (Figure 1). The SLB contained one part of negatively charged phospholipids (1,2-dioleoyl-*sn*-glycero-3-phospho-L-serine, DOPS) and four parts of neutral phospholipids (1,2-dioleoyl-*sn*-glycero-3-phosphocholine, DOPC). The chosen ratio is similar to the composition of the inner leaflet of neuronal membranes, which is typically enriched with negatively charged phospholipids in the range of 15−30 mol %.[40−42] Similar lipid ratios have been used in other protein aggregation studies and found to form well mixed bilayers containing few defects, while still retaining the negative charge necessary to encourage protein adsorption.[43,44] Indeed, the SLBs used in this study did not display obvious defects or other inhomogeneities. This finding is corroborated by previously performed experiments based on fluorescence recovery after photobleaching (FRAP).[44]

The total protein concentration of the bulk solution was as low as 1 nM in normal phosphate-buffered saline (1 × PBS, ionic strength = 166 mM). Time-resolved SAF imaging shows that both donor and acceptor labeled α-Syn proteins rapidly adhere to the SLB and form aggregates within the first measurement frame of 1 h (Figure 1). In the SAF measurements shown in Figure 1, nonaggregated proteins are invisible in the acceptor image because the laser of the optical setup (emission 635 nm) does not excite acceptor fluorophores directly (absorption max 750 nm).[39] Hence, the acceptor image shows exclusively aggregates, that is, proteins that are associated with at least one other protein, while in the donor image (D) aggregated plus nonaggregated proteins are detected. On the basis of the donor and the acceptor images, a FRET image can be calculated showing the energy transfer efficiencies in every point (Figure 1, right).

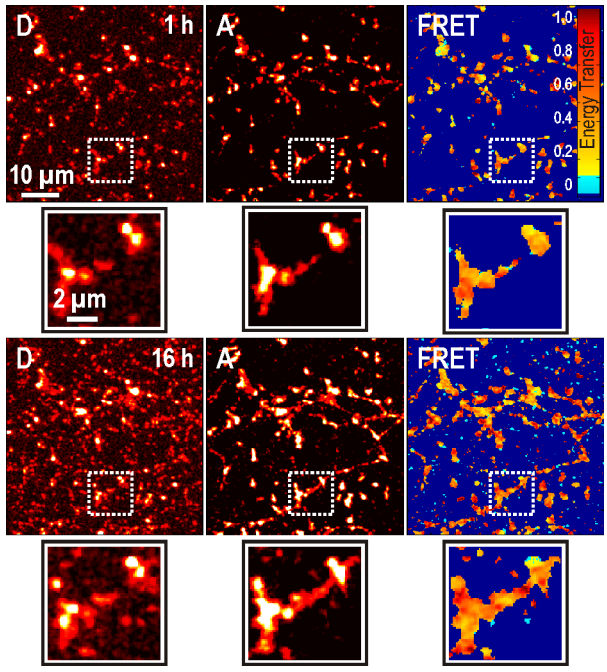

Figure 1. α-Syn aggregation on the SLB. Donor (D), acceptor (A), and FRET images of the same scanned areas acquired after 1 h (top row) and 16 h (bottom row) of exposure to a mixture of donor and acceptor labeled α-Syn (0.5 nM each) on the SLB. The section marked by a dashed line is magnified in the boxes underneath each image. FRET signals arise solely from aggregated α-Syn molecules.

Figure 1 (top) shows the initial adsorption and aggregation state of α-Syn proteins on the SLB after an incubation time of 1 h. Protein aggregates appeared to be randomly distributed, covering most of the available surface. Additionally, nonaggregated α-Syn proteins are present together with the aggregates and can be found across the entire surface (see magnification of the donor image in Figure 1). However, these nonaggregated proteins do not emit any measurable signal into the acceptor channel and can therefore efficiently be differentiated from aggregated proteins. To this end the FRET technique is a highly valuable tool to avoid misinterpretations that could arise from nonaggregated proteins in conventional microscopy. We incubated the surface with α-Syn (bulk concentration 1 nM) for several hours while maintaining a constant protein supply using a constant buffer flow. After 16 h, most aggregates that had already arisen within the first hour have grown into larger elongated α-Syn aggregates (Figure 1, bottom). A dendrite-like morphology was observable in many spots, possibly resulting from the overlay of distinct aggregates or fibril bundles.[45,46]

Taking into account that the spatial resolution of the 3D-SAF microscope is in the range of 300 nm, the sizes of the observable aggregates varied from a few nanometers (subdiffraction range) in the initial stages of aggregation to a few micrometers in length after longer incubation times. This is in agreement with the commonly observed size ranges of α-Syn oligomers, protofibrils, and fibrils.[7,13,14,26,47−50] At the end of the experiment, we checked that the lipid bilayer was not removed due to α-Syn adsorption and aggregation by staining the surface with the membrane intercalating fluorophore Cellmask™. Indeed, an intense fluorescence increase indicated

dx.doi.org/10.1021/cn3001312 | ACS Chem. Neurosci. 2013, 4, 408−417

that the bilayer was still present, and even if damaged by aggregation, it was not removed in its entirety during the experiment (see Supporting Information, Figure S1).

On-Surface Growth of α-Syn Aggregates. A quantitative approach to monitor the process of aggregate growth *in situ* consists of the sequential FRET experiment presented in Figure 2. First, only donor labeled α-Syn at a bulk concentration of 0.5

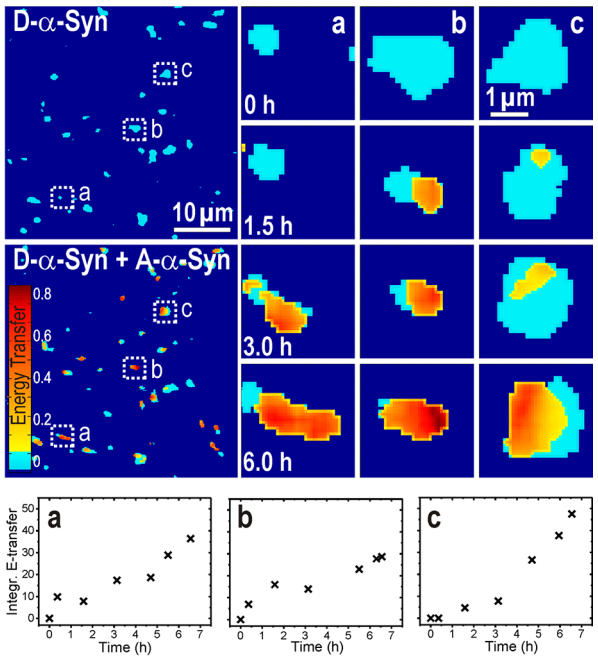

Figure 2. Monitoring the α-Syn aggregation on the SLB. First, only donor (D) labeled α-Syn was applied to the surface followed by addition of only acceptor (A) labeled α-Syn. Light blue color indicates no energy transfer, that is, only donor fluorescence. The appearance of energy transfer (yellow to red color) results from aggregation events. The time-resolved energy transfer of each of the three aggregates indicated by a, b, and c is shown on the right as images. In addition, the graphs labeled accordingly show the integrated energy transfers of each of the three aggregates versus time (bottom).

nM was applied to the surface. Then, only acceptor labeled α-Syn at the same concentration was additionally added. The increase of the fluorescence intensity in the acceptor image suggests that α-Syn monomers or small oligomers thereof bind on top of surface bound α-Syn aggregates since only in that case can FRET signals be detected (yellow to red areas in Figure 2). The energy transfer values of three arbitrarily chosen donor labeled aggregates were extracted from the scan image and monitored over time while acceptor labeled proteins were constantly supplied in solution (Figure 2a,b,c). At different points in time, the energy transfer efficiencies integrated over all pixels belonging to one aggregate were plotted, leading to the aggregation kinetics presented in Figure 2 (bottom). In all three cases, these kinetics indicate a continuous growing of α-Syn aggregates. We could not observe a stepwise increase or significant intensity jumps that would imply the deposition of larger aggregates from the solution to the surface. The latter scenario was previously observed in the case of BSA clusters that had formed through an in-solution process.[39] We therefore exclude that in the conditions studied α-Syn forms aggregates or oligomers in solution at nanomolar concentrations. This finding is in agreement with numerous previous studies demonstrating that fibril formation of α-Syn in solution only takes place at micromolar concentrations (100−300 μM).[2,6,30,51,52] Thus, the α-Syn aggregates observed in the present study underlay an on-surface growth mechanism regardless of whether a lipid bilayer (presented in Figure 2) or a bare glass surface (presented in Supporting Information, Figure S2) was used. The bulk protein concentration of α-Syn that was needed to trigger the formation of surface aggregates was as low as 1 nM on the SLB and 0.2 nM on the glass surface. It should be noted that the α-Syn nucleation event was not induced by impurities adsorbed to the surface or present in the bulk solution since all surfaces were thoroughly cleaned and buffers as well as protein solutions were filtered through 0.22 μm pore size filters. As shown in our previous works, treated glass surfaces constantly showed quantitatively reproducible and homogeneous protein binding characteristics.[53,54] In the case of SLBs, the process of protein adsorption and aggregation in the presence of the bilayer is widespread and appears very similar to that happening on a bare glass surface (see Figure S2 in the Supporting Information). Thus, even if we cannot completely resolve the influence of potential structural surface inhomogeneities, it is obvious from our experimental results that α-Syn aggregation is induced by the presence of a negatively charged uniform surface, either glass or SLB, and not by impurities or bilayer defects with direct access to the glass substrate underneath.

In-Solution Growth of Surface-Tethered α-Syn Aggregates. The SAF channel of the microscope restricted the observations to a region close to the SLB interface since the collected emitter intensity decays rapidly with its distance from the surface. Objects that are more than 100−200 nm away from the surface are not detected.[37] Nevertheless, features that extend deeper from the interface into the bulk solution can still be detected using an additional optical channel, which collects the undercritical angle fluorescence (UAF) of labeled biomolecules. Practically, the UAF channel allows for conventional confocal imaging up to ∼2.5 μm deep into the solution.[37] By combination of the fluorescence intensities measured with these two channels, UAF and SAF, surface images with height information of subdiffraction *z*-resolution can be generated, a technique that was recently introduced as 3D-SAF microscopy.[38]

The strength of 3D-SAF microscopy was exploited to distinguish surface features with different extensions in the *z*-direction. The 3D-SAF measurements reveal that in addition to the persistently surface bound aggregates observed so far, extended surface-tethered structures protruding between 1 and 3 μm or even deeper into the solution were present (Figure 3). At the low concentrations examined in this study, this outgrowth from the SLB plane was clearly more pronounced when the ionic strength conditions were reduced by a factor of 10 (refer to Figure S3 in the Supporting Information for a comparison of the outgrowth of aggregates grown at 1× and 0.1× PBS). In detail, Figure 3a shows a supported lipid bilayer incubated for 20 h with a solution of α-Syn at a starting concentration of 1 nM. The SAF images (Figure 3, center column) show exclusively those aggregates or parts thereof that are in close proximity to the lipid interface whereas the corresponding UAF images (Figure 3, left column) show additionally those aggregates that protrude into the bulk solution. Calculating the ratio between signals detected by the UAF and the SAF channel allowed us to generate images containing height information (Figure 3, right column). Low

dx.doi.org/10.1021/cn3001312 | ACS Chem. Neurosci. 2013, 4, 408−417

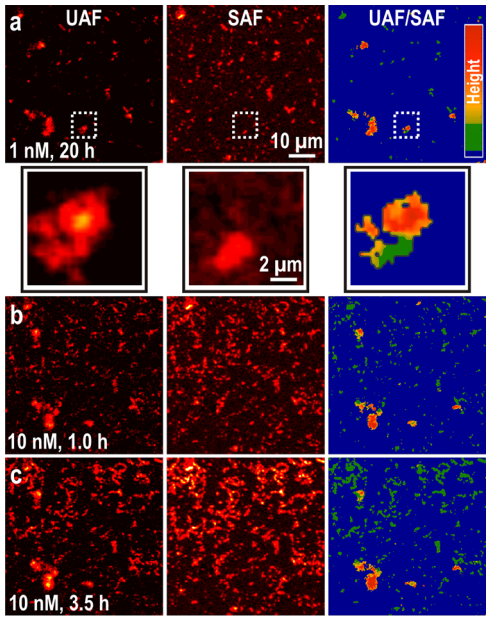

Figure 3. Supercritical angle fluorescence (SAF) and undercritical angle fluorescence (UAF) detection of protein aggregation. (a) The α-Syn concentration is 1 nM in a buffer composed of 0.1 × PBS (having an ionic strength of 16.6 mM). The UAF-to-SAF-ratio shows the protrusion of the aggregates into the bulk as highlighted by the color code in the z-axis from green (close to the SLB) to red (1−3 μm away from the SLB). In the insets, magnifications of single selected aggregates are highlighted. Images shown in b and c were recorded 1 and 3.5 h after increasing the concentration to 10 nM (0.1 × PBS).

ratios, visualized by green color, correspond to entities that are close to the surface whereas high ratios, visualized by red color, correspond to structures further away from the surface. UAF-to-SAF-ratio images cannot be obtained at the same time as FRET images. Therefore α-Syn proteins shown in Figure 3 were exclusively labeled with one type of fluorophore (DY-647). These images indicate that there are two distinct types of aggregates. Type 1 consists of entirely surface bound aggregates being completely flat as is seen from the low UAF-to-SAF ratios in Figure 3, right column (green color). Type 2 refers to those aggregates that are also tethered to the surface with one end but additionally protrude deeper into the bulk solution with their other end resulting in high UAF-to-SAF ratios (red color in Figure 3, right column). For a better visualization of the aggregates' growth, we accelerated this process by increasing the bulk concentration of α-Syn by a factor of 10. As can be observed clearly from Figure 3, rows b and c, both types of protein aggregates continued to grow. In particular, type 1 aggregates are observed to preferably grow at the end of the clusters leading to elongated structures that remain attached to the surface. Thus, for this type of aggregate monomer addition requires both preformed aggregate plus the surface. By contrast, type 2 aggregates grow extensively in the bulk solution (seen in the UAF images in Figure 3), thus monomer addition requires only the preformed aggregate but no surface. The transition of type 1 into type 2 aggregate might be a rare event because only a small number of all surface bound aggregates show the type 2 characteristics.

Surface-Bound α-Syn Aggregates Contain Amyloid Structures. To characterize the structural properties of the bound aggregates, we further incubated the surfaces with thioflavin T (ThT). ThT is routinely used to test for the presence of amyloids, since its fluorescence is wavelength shifted and greatly increased upon binding to amyloid species.[7,55] Indeed, after incubation of α-Syn at low bulk concentrations (1 nM, 0.1 × PBS) for 20 h, the presence of amyloid fibrils on the SLB was confirmed by the observation of positive ThT staining imaged by epifluorescence microscopy (Figure 4). The time span of 20 h ensures that a reasonable

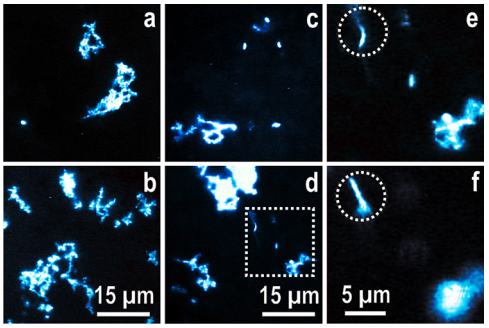

Figure 4. Epifluorescence microscopy images of α-Syn amyloid fibrils grown at 1 nM, 0.1 × PBS on a SLB. Extended curly structures (a, b) and short elongated surface bound aggregates (c) grown for 20 h respond to ThT staining. Images e and f present the same section (magnification from image d) with the focal plane being set on the surface and a few micrometers inside the bulk solution, respectively.

number of α-Syn aggregates can be detected. It does not mean, however, that all aggregates are 20 h old because lag times for nucleation and growth can vary tremendously (refer to Figure S4 in the Supporting Information for α-Syn aggregates at an early aggregation stage). Since the binding of ThT to extended cross-β-sheet structures results in a well-established enhancement and red shift of the fluorescence emission maximum,[55] the emission was recorded at wavelengths around 483 nm to match the ThT emission spectrum in its bound state. Large twisted structures (Figure 4a,b) side by side with small elongated surface bound aggregates (Figure 4c) were stained by the ThT fluorophore. The bulk solution itself showed no measurable fluorescence increase indicating that amyloid fibrils under the applied conditions are exclusively found at the surface of the SLB. However, there are amyloid fibrils protruding into the bulk solution as presented in Figure 4 d (and magnified in Figure 4e,f). By adjustment of the focal plane precisely to the surface only the lower end of the encircled feature is clearly resolved (Figure 4e). In order to image the upper end of the same feature, the focus has to be shifted upward into the solution confirming that this structural entity has an unambiguous extension in the z-direction (Figure 4f). Similar morphologies of α-Syn aggregates grown at micromolar concentrations on lipid bilayers were observed by electron microscopy[25] and epifluorescence microscopy.[26,56] The ThT staining indicates that α-Syn aggregates grown at nanomolar concentrations on the surface are of amyloid-like nature because this dye is known to specifically bind to cross-β sheets found in amyloids.[57,58] In addition, we performed an antibody stain using a conformational specific anti-amyloid antibody (OC).[59] For this experiment, we employed unlabeled α-Syn protein and observed extensive antibody binding, indicative of the presence of amyloid-like structures (Figure S5 in the Supporting Information). Since label-free α-Syn followed the same aggregation process as the acceptor or donor labeled protein, the influence of the fluorophores can be considered

dx.doi.org/10.1021/cn3001312 | ACS Chem. Neurosci. 2013, 4, 408−417

negligible, in line with what was reported in other studies.[26,29,44,49]

Surface-Tethered α-Syn Aggregates Are Mobile at Their Solution-Protruding End. To extract more details on the properties of the α-Syn aggregates including their surface anchoring points, magnifications of a few examples of extended aggregates of type 2 grown at low bulk concentrations are presented in Figure 5. Interestingly, these examples showed

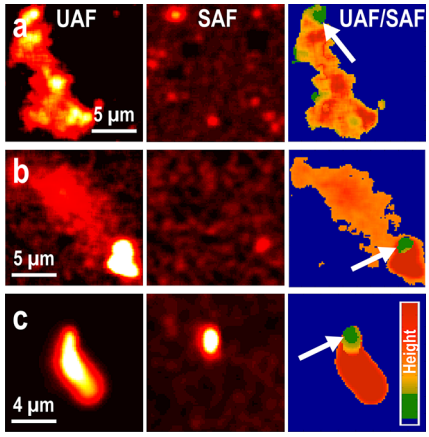

Figure 5. Large aggregates protrude deep into the bulk solution. The aggregates were grown at bulk concentrations of 1 nM on a SLB (a) or 10 nM on a glass surface (b, c). UAF detection shows an image of the structures up to 2.5 μm deep into the solution (left column). SAF detection shows images of these fibrils in close vicinity (~100−200 nm) to the surface (middle column). The UAF-to-SAF-ratio images (right column) visualize the anchoring points of the amyloid fibrils (white arrows).

that extended α-Syn aggregates are typically tethered to the surface via small anchoring points (green areas in Figure 5, right column). In particular the UAF-to-SAF-ratio images highlighted that the observed structures are small at the interface and became increasingly bulky also in lateral dimensions at higher *z*-positions. Regardless of the relatively small anchoring area, the aggregates were extraordinarily tightly tethered to the surface. Practically, they almost never changed their position on the surface over the whole observation period (up to several days). Interestingly, this feature was independent of the surface utilized, whether a lipid bilayer (Figure 5a) or a bare glass surface (Figure 5b,c) was used. When the lipid layer was removed by rinsing with a detergent solution (2% SDS), the surface tethered α-Syn aggregates remained at their positions (see Supporting Information, Figure S6). This finding strongly suggested that even if α-Syn aggregates started growing on the surface of the SLB, they eventually penetrated the lipid bilayer and attached to the glass support underneath.

By increasing the flow rate within the measuring cell (0.42 mm/s), one can apply moderate shear forces to the aggregates (Figure 6). Depending on the flow direction, their upper end bent to the left or to the right (colored in red and in pink in Figure 6), while their lower end was attached to the surface (green areas in Figure 6). We found that extended α-Syn aggregates could be repeatedly moved back and forth for an unlimited number of cycles. Even extensive rinsing with protein-free buffer did not remove or diminish the protein aggregates suggesting an irreversible and tight surface binding. Only upon strongly increasing the flow velocity (>3 mm/s)

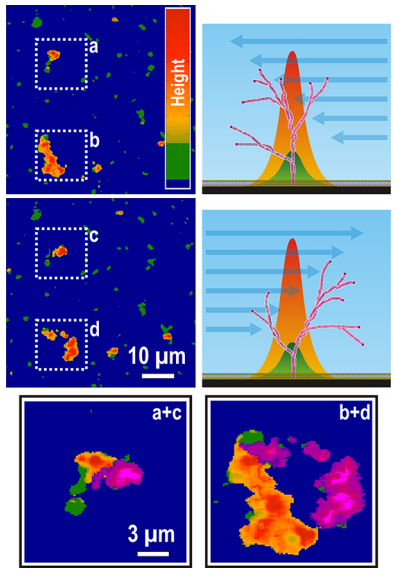

Figure 6. Bending of extended amyloid fibrils. Scan images were recorded with the buffer flowing from right to left (up) and from left to right (middle), which moves the fibrils protruding deep into the solution. The images in the third row represent overlays of the marked regions with the orange color referring to a buffer flow from right to left and the violet color referring to a buffer flow from left to right. The surface anchoring points (green) do not move. Refer to Supporting Information, Figure S7, for an analogous experiment conducted on the bare glass surface.

were the shear forces potent enough to remove the aggregates from the surface (data not shown).

Two Different Growing Mechanisms of Type 1 and Type 2 α-Syn Aggregates. Exposing a solution of α-Syn monomers to a hydrophilic surface, either a negatively charged lipid bilayer or a negatively charged glass surface, prompted the growth of surface bound aggregates. In Figure 7, we compare aggregate growth on the two different surfaces at low ionic strength (0.1 × PBS) and at α-Syn bulk concentrations of 10 nM on the SLB (column a, b) and only 0.2 nM on glass (column c, d). Indeed, as visible in the representative time series, we observed no striking difference between aggregate growth in *z*-dimension on the two surfaces.

Using the opportunities provided by 3D-SAF microscopy, we could identify two distinct types of α-Syn aggregates: type 1, flat and entirely surface bound, or type 2, surface tethered only at one end and protruding into the bulk solution at the other end. Type 1 aggregates grew by monomer addition along the plane persistently in contact with the surface. Type 2 aggregates grew perpendicularly to the plane; even though surface tethered, they protruded in *z*-direction into the bulk solution. Both types of protein aggregates started as surface-mediated processes, remaining anchored tightly to the plane throughout their growing process and are amyloid in nature, as indicated by positive ThT staining and amyloid specific antibodies. Nevertheless, in this study we identified some striking differences in the lag phase and kinetics of growth of the different types.

The process of aggregation along the surface plane resulting in type 1 aggregates had virtually no lag phase, beginning immediately when the hydrophilic surface was exposed to a solution of α-Syn monomers. The aggregation proceeded at moderate growing rates. Type 1 aggregates displayed a linear or dendrite-like morphology of a few micrometers in length after 10−20 h.

dx.doi.org/10.1021/cn3001312 | ACS Chem. Neurosci. 2013, 4, 408−417

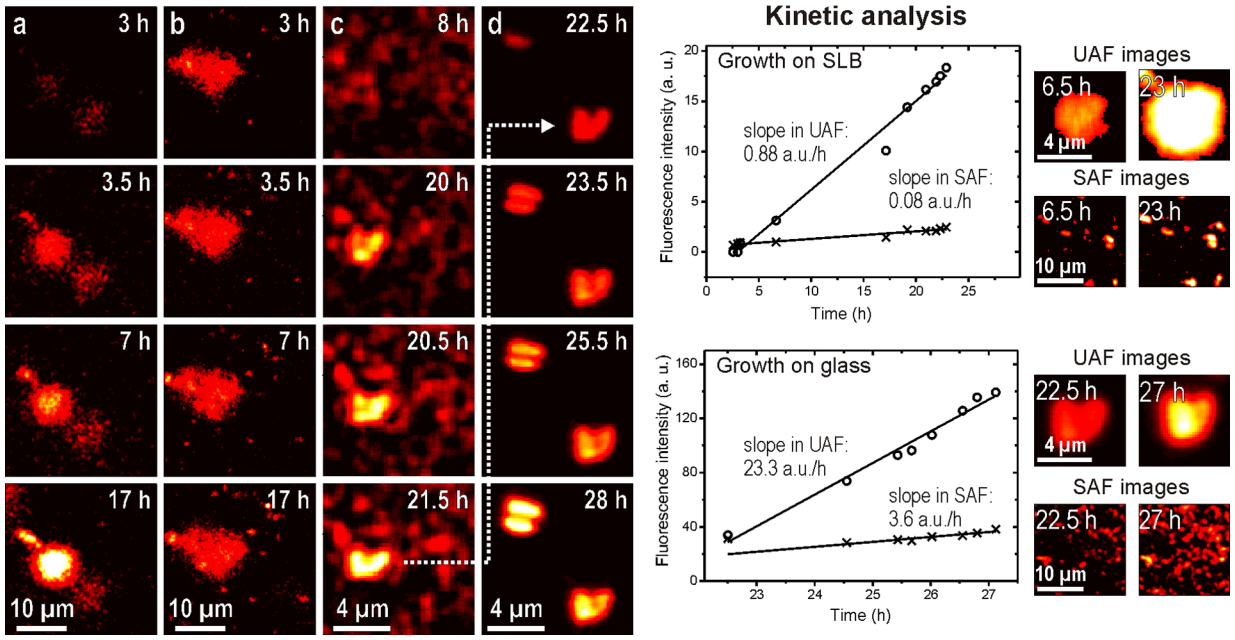

Figure 7. α-Syn aggregation process on a glass and a SLB surface. Aggregates presented in columns a and b were grown in 0.1 × PBS on a SLB at a concentration of 10 nM. Aggregates presented in column c and d were grown in (0.1 × PBS) on the glass surface at a concentration of only 0.2 nM. Kinetic plots (middle) present α-Syn aggregation in the z-direction (monitored by UAF) and α-Syn aggregation along the surface plane (monitored by SAF). Images on the right show the surface sections evaluated for the kinetic analyses.

By contrast, the growth of extended (type 2) α-Syn aggregates away from the surface typically started suddenly after a lag time of several hours and proceeded considerably faster than the type 1 growth. The resulting aggregates protruded up to several micrometers deep into the solution and typically accommodated several thousands of α-Syn monomers, as inferred from their fluorescence intensity.[39] Compared with their overall spatial and axial dimensions, these entities are tethered to the surface via a small anchoring site, which enables them to bend at their mobile end in the buffer flow. While their growth started as a surface-mediated process, it later proceeded in the bulk solution as a surface-independent process, caused only by further addition of monomers. This second type of amyloids could possibly arise from the transition of a type 1 aggregate or a part thereof as a result of significant structural or conformational reorganization. The total number of type 2 aggregates did not vary significantly with time; therefore it is reasonable to consider this transition as a relatively rare event. The type of growing mechanism is locally defined by the type of aggregate present. If a type 1 aggregate is present, a type 1 growing mechanism is observed, and if a type 2 aggregate is present, a type 2 growing mechanism is observed.

By recording the total fluorescence intensity emitted into the UAF channel of the 3D-SAF microscope, we quantified the aggregation process of type 2 aggregates. Similarly, the growth of type 1 was obtained by recording the total fluorescence intensities emitted into the SAF channel. Comparing the two growth rates, we found that on both SLB and glass surfaces, type 2 aggregates grew faster than type 1 by about 1 order of magnitude (Figure 7, see plots). On the lipid bilayer model, the initial growth rate of the selected type 2 aggregate presented in column a of Figure 7 was 11 times greater than the mean growth rate of the surface bound (type 1) aggregates. A similar behavior was observed on glass, where the growth of the selected type 2 aggregates (columns c, d, Figure 7) was 6.5 times greater than the type 1 aggregates. It is apparent that the type 2 aggregates observed resemble α-Syn fibrils grown at high bulk concentrations in solution, which typically show a variable and stochastic lag phase followed by a rapid elongation process.[7,13,14,50,60]

Elongated, linear, or dendrite-like fibrils of length up to several micrometers were frequently reported in the context of α-Syn fibrillation.[7,13,14,50] In addition, aggregation mechanisms for amyloidogenic proteins at interfaces in agreement with our observations are comprehensively described in the literature.[61,62] For instance, Zhu et al. reported two distinct on-surface aggregation mechanisms for the amyloidogenic protein SMA predominantly differing in their growth rates.[62] Recently, Giehm et al. have observed a continuous accretion during the formation of α-Syn aggregates on SDS micelles rather than a rate-limiting accumulation of a distinct nucleus,[61] which is comparable with the observed growth of the type 1 aggregate in our study. In addition to those studies, however, we show here that α-Syn molecules can aggregate on surfaces at bulk concentrations of 1 nM and below, while amyloid fibril formation by α-Syn has been observed in solution only at higher micromolar concentrations. In our study, the initial aggregation event takes place on hydrophilic surfaces such as partially negatively charged planar lipid bilayers, which resemble polar cellular membranes. This is particularly important considering that most previous cases of *in vitro* α-Syn aggregation are believed to be triggered by reactions on physiologically irrelevant hydrophobic interfaces.[30]

In addition, the existence of at least two distinct species may aid in understanding the numerous *in vitro* studies in which amyloidogenic proteins are found to arise after a highly variable lag time. From our findings we can speculate that type 1 aggregates could grow on the glass walls of a measuring cell during the lag time of an *in vitro* experiment. Stochastically, some type 1 clusters could transition into type 2 aggregates that display a drastically accelerated growth rate. Unlike type 1 aggregates, which are entirely surface-bound, type 2 amyloids

dx.doi.org/10.1021/cn3001312 | ACS Chem. Neurosci. 2013, 4, 408−417

are elongated and only partially surface bound and could be removed by a shear force (for instance by stirring). It can be expected that fragmentation of type 2 aggregates will further speed up the aggregation process since their elongation and further growth is surface independent. This is in agreement with the observation that fibrillization of α-Syn in solution is accelerated by stirring.[30,63]

***In Vivo* Aggregation of α-Syn Is Hindered in Healthy Neurons.** In the current discussion about the origin of amyloidogenic disorders, it is frequently asked how it is possible that aggregates and fibrils made of amyloidogenic proteins can form *in vivo* given that the physiological concentration is obviously much lower than the critical concentration necessary to trigger aggregation.[2,16,18−20] As a consequence, research activities in this field focus on either aggregation-inducer molecules,[64,65] aggregation-inducing surfaces,[22,23,25,26,30] or cellular mechanisms responsible for a local increase of the concentration levels of the amyloidogenic proteins of interest.[2,19−21] The present study demonstrated that α-Syn aggregation on negatively charged lipid bilayers or glass substrates is a surface-induced process even at low nanomolar concentrations, which is up to 4 orders of magnitudes below the physiological concentration of α-Syn. The nucleation process was found to essentially take place on the surface. The following growth of these aggregates, however, can be directed along the surface or away from it. From a biological point of view, this finding raises the question of what cellular mechanism ensures that α-Syn does not aggregate *in vivo* under nonpathological conditions. Possible scenarios include a prevention of the adsorption of α-Syn to lipid interfaces or a hindrance of conformational transitions. The deterioration of these aggregation-preventing mechanisms upon aging could lead to the onset of Parkinson's disease or other neurodegenerative conditions.

METHODS

Protein Expression and Labeling. The protocol for wild-type α-Syn expression and purification has been described previously.[44] In brief, *Escherichia coli* BL21(DE3)-Star competent cells (Stratagene) were transformed with the appropriate plasmid. The bacteria were grown at 37 °C, and protein expression was achieved inducing at an A_{600} of around 0.8 to 1 with 1 mM isopropyl-1-thio-β-D-galactopyranoside (IPTG) at 37 °C overnight. The bacterial lysate was heated for 10 min at 70 °C and pelleted for 30 min at 14000*g*. Subsequently, the protein was precipitated and purified through several cycles of resuspension, dialysis, and precipitation.

Fluorescent labeling of α-Syn was achieved by adding 250 μL of α-Syn (3.5 mg/mL in phosphate-buffered saline, pH 9.3) solution to 0.2 mg of lyophilized DY-647-NHS (donor) and by adding 100 μL of α-Syn solution to 0.2 mg of Cy7-NHS (acceptor). The reactions took place overnight at room temperature leading to final dye-to-protein ratios of 0.49 (DY647-α-Syn) and 0.45 (Cy7-α-Syn), as determined by UV/vis spectroscopy using the following extinction coefficient for α-Syn: ε = 5600 M^{-1} cm^{-1} (λ_{max}(α-Syn) = 275 nm).[66] This means on average around every second protein is labeled either with a donor or with an acceptor fluorophore. Labeled α-Syn was separated from unbound dye and other potential impurities via size exclusion chromatography using a SuperdexTM 200 10/300 GL column (Amersham). Aliquots of labeled protein were lyophilized and stored at −20 °C for up to 6 months. Solutions of the protein were stored for a maximum of 2−4 weeks at 4 °C in the dark at 30 μM concentration in PBS and filtered through 0.22 μm pore membrane filters prior to usage. Size exclusion chromatography did not reveal significant changes during the storage interval and experimental results were independent of the storage time of our samples. Double distilled water and membrane filtered (0.22 μm) buffer was used throughout all preparation steps.

Glass Surface Preparation. Standard microscopy glass coverslips (Menzel, Germany) were used for all experiments described herein. To obtain equilibrated and homogeneous surfaces, all coverslips had been immersed in a mild detergent solution (Deconex, 0.2%) for at least 7 days. This method was proven very efficient for ensuring quantitatively reproducible protein adsorption kinetics.[53,54] Prior to use, the coverslips were extensively washed with substantial amounts of ethanol and subsequently double distilled water to remove traces of the detergent. For experiments conducted on the glass surface, these coverslips were used directly, whereas for experiments on the SLB, they were further modified as described in the following paragraph.

Lipid Bilayer Formation. Negatively charged lipids, 1,2-dioleoyl-*sn*-glycero-3-phospho-L-serine (DOPS), and net neutral lipids, 1,2-dioleoyl-*sn*-glycero-3-phosphocholine (DOPC), were supplied in chloroform and used as received (Avanti Polar Lipids). A mixture of DOPC and DOPS (4:1) was stirred under reduced pressure in order to remove the solvent. The resulting solid was placed under high vacuum (1 mbar) overnight to remove any traces of chloroform. The dried lipids were resuspended in membrane buffer (NaCl (100 mM), $CaCl_2 \cdot H_2O$ (3 mM), Tris (100 mM), pH 7.5) and repeatedly extruded through a porous membrane filter (pore size 100 nm) in order to produce unilamellar vesicles with a homogeneous size distribution. Solutions of ULV (0.1 mg/mL) in membrane buffer were passed over the hydrophilic glass surface leading to fusion into a supported lipid bilayer (SLB). Prior to use, the glass coverslips had been cleaned by immersion in a mild detergent solution (Deconex, 0.2%) for several days followed by extensive ethanol and water rinse.

3D-SAF and FRET Imaging. Images of fluorescently labeled α-Syn aggregates were recorded with a custom-made scanning microscope allowing detection of the supercritical angle fluorescence (SAF) and the undercritical angle fluorescence (UAF) of an emitter simultaneously.[37] The SAF channel only detects fluorophores in close proximity to the surface (∼100−200 nm) and efficiently rejects the fluorescence from the bulk solution using a parabolic mirror as the decisive optical element.[37] The UAF channel detects the fluorescence from deeper inside the solution (∼2.5 μm) using conventional confocal optics. A detailed description of the optical setup is provided in ref 37. Surface-confined FRET imaging was achieved by splitting and separating the detection of the fluorescence emission of the SAF channel into donor and acceptor signals via a dichroic mirror at 730 nm. All measurements were conducted by passing buffered solutions of protein over the SLB or the bare glass surface through the flow cell at a constant pump rate of 250 μL/min (0.42 mm/s) unless otherwise stated. This flow rate is clearly slow enough to have no effect on the supported lipid bilayer integrity.

Raw scan images are presented as measured using appropriate linear scaling for the signal intensities. All calculated FRET images and UAF-to-SAF-ratio images were subjected to a nearest neighbor average smoothing and background subtraction in order to avoid noisy images. Donor and acceptor images were corrected for background emission and for the crosstalk between the two detection channels prior to calculating FRET images.[67] Calculated images were presented with a blue background in order to differentiate them from raw images. Note that the background subtraction in all images is based on a fixed intensity threshold. In the case that the intensity of some pixels falls under this threshold due to photobleaching or energy transfer effects, this can lead to a seeming but not real decrease in the size of α-Syn aggregates (see Figure 2b). The shown images are selected representative images from time-lapse experiments which were conducted at varying time intervals because the applied (non-commercial) setup does not contain the option of a software-controlled time-lapse measurement.

ThT Staining, Epifluorescence Microscopy. A strongly diluted solution of thioflavin T (ThT) in buffer (0.1 × PBS) was pumped through the flow cell over the SLB, which had been exposed to α-Syn for a sufficiently long time. The flow cell was mounted carefully on a Nikon Eclipse TE2000 microscope, and images were recorded using

438/24 and 483/32 band-pass filters for excitation and emission, respectively.

The alternative method for amyloid staining based on Congo Red birefringence was not applied in this work because it is only evident when the specimen thickness is constant and in the range of 8−10 μm, well above the observed morphology.[68] In addition, the staining process would destroy the bilayer because it includes washes in ethanol or high pH and salt buffers. Fixing the sample in formaldehyde, however, may alter it and therefore question the conclusions.

■ ASSOCIATED CONTENT

Supporting Information

Further fluorescence microscopy images and schemes presenting additional details on α-Syn aggregation. This material is available free of charge via the Internet at http://pubs.acs.org.

■ AUTHOR INFORMATION

Corresponding Authors

*Roland Riek: tel. +41- (0)44-6326139, e-mail address: roland.riek@phys.chem.ethz.ch.

*Stefan Seeger: fax +41-(0)44-6356813, tel. +41-(0)44-6354451, e-mail address: sseeger@pci.uzh.ch.

Author Contributions

M.R., A.S., N.R., and D.V. designed, executed, and interpreted the experiments. E.L. produced the applied samples. M.R. wrote the manuscript. A.S., N.R., D.V., R.R., and S.S. contributed to the text of the manuscript. R.R. and S.S. initiated and organized the project.

Funding

This work was supported by the Swiss National Science Foundation (SNSF) and the ETH Zurich.

Notes

The authors declare no competing financial interest.

■ REFERENCES

(1) Cabin, D. E., Shimazu, K., Murphy, D., Cole, N. B., Gottschalk, W., McIlwain, K. L., Orrison, B., Chen, A., Ellis, C. E., Paylor, R., Lu, B., and Nussbaum, R. L. (2002) Synaptic vesicle depletion correlates with attenuated synaptic responses to prolonged repetitive stimulation in mice lacking alpha-synuclein. *J. Neurosci. 22*, 8797−8807.

(2) Shtilerman, M. D., Ding, T. T., and Lansbury, P. T. (2002) Molecular crowding accelerates fibrillization of alpha-synuclein: Could an increase in the cytoplasmic protein concentration induce Parkinson's disease? *Biochemistry 41*, 3855−3860.

(3) Cookson, M. R. (2005) The biochemistry of Parkinson's disease. *Annu. Rev. Biochem. 74*, 29−52.

(4) Cookson, M. R., and van der Brug, M. (2008) Cell systems and the toxic mechanism(s) of alpha-synuclein. *Exp. Neurol. 209*, 5−11.

(5) Vilar, M., Chou, H. T., Luhrs, T., Maji, S. K., Riek-Loher, D., Verel, R., Manning, G., Stahlberg, H., and Riek, R. (2008) The fold of alpha-synuclein fibrils. *Proc. Natl. Acad. Sci. U.S.A. 105*, 8637−8642.

(6) Conway, K. A., Harper, J. D., and Lansbury, P. T. (1998) Accelerated in vitro fibril formation by a mutant alpha-synuclein linked to early-onset Parkinson disease. *Nat. Med. 4*, 1318−1320.

(7) Conway, K. A., Harper, J. D., and Lansbury, P. T. (2000) Fibrils formed in vitro from alpha-synuclein and two mutant forms linked to Parkinson's disease are typical amyloid. *Biochemistry 39*, 2552−2563.

(8) Singleton, A. B., Farrer, M., Johnson, J., Singleton, A., Hague, S., Kachergus, J., Hulihan, M., Peuralinna, T., Dutra, A., Nussbaum, R., Lincoln, S., Crawley, A., Hanson, M., Maraganore, D., Adler, C., Cookson, M. R., Muenter, M., Baptista, M., Miller, D., Blancato, J., Hardy, J., and Gwinn-Hardy, K. (2003) Alpha-synuclein locus triplication causes Parkinson's disease. *Science 302*, 841−841.

(9) Krüger, R., Kuhn, W., Muller, T., Woitalla, D., Graeber, M., Kosel, S., Przuntek, H., Epplen, J. T., Schols, L., and Riess, O. (1998) Ala30Pro mutation in the gene encoding alpha-synuclein in Parkinson's disease. *Nat. Genet. 18*, 106−108.

(10) Polymeropoulos, M. H., Lavedan, C., Leroy, E., Ide, S. E., Dehejia, A., Dutra, A., Pike, B., Root, H., Rubenstein, J., Boyer, R., Stenroos, E. S., Chandrasekharappa, S., Athanassiadou, A., Papapetropoulos, T., Johnson, W. G., Lazzarini, A. M., Duvoisin, R. C., DiIorio, G., Golbe, L. I., and Nussbaum, R. L. (1997) Mutation in the alpha-synuclein gene identified in families with Parkinson's disease. *Science 276*, 2045−2047.

(11) Zarranz, J. J., Alegre, J., Gomez-Esteban, J. C., Lezcano, E., Ros, R., Ampuero, I., Vidal, L., Hoenicka, J., Rodriguez, O., Atares, B., Llorens, V., Tortosa, E. G., del Ser, T., Munoz, D. G., and de Yebenes, J. G. (2004) The new mutation, E46K, of alpha-synuclein causes Parkinson and Lewy body dementia. *Ann. Neurol. 55*, 164−173.

(12) Apetri, M. M., Maiti, N. C., Zagorski, M. G., Carey, P. R., and Anderson, V. E. (2006) Secondary structure of alpha-synuclein oligomers: Characterization by Raman and atomic force microscopy. *J. Mol. Biol. 355*, 63−71.

(13) Lashuel, H. A., Petre, B. M., Wall, J., Simon, M., Nowak, R. J., Walz, T., and Lansbury, P. T. (2002) Alpha-synuclein, especially the Parkinson's disease-associated mutants, forms pore-like annular and tubular protofibrils. *J. Mol. Biol. 322*, 1089−1102.

(14) Smith, D. P., Tew, D. J., Hill, A. F., Bottomley, S. P., Masters, C. L., Barnham, K. J., and Cappai, R. (2008) Formation of a high affinity lipid-binding intermediate during the early aggregation phase of alpha-synuclein. *Biochemistry 47*, 1425−1434.

(15) Conway, K. A., Rochet, J. C., Bieganski, R. M., and Lansbury, P. T. (2001) Kinetic stabilization of the alpha-synuclein protofibril by a dopamine-alpha-synuclein adduct. *Science 294*, 1346−1349.

(16) Rochet, J. C., and Lansbury, P. T. (2000) Amyloid fibrillogenesis: Themes and variations. *Curr. Opin. Struct. Biol. 10*, 60−68.

(17) Wood, S. J., Wypych, J., Steavenson, S., Louis, J. C., Citron, M., and Biere, A. L. (1999) Alpha-synuclein fibrillogenesis is nucleation-dependent - Implications for the pathogenesis of Parkinson's disease. *J. Biol. Chem. 274*, 19509−19512.

(18) Harper, J. D., and Lansbury, P. T. (1997) Models of amyloid seeding in Alzheimier's disease and scrapie: Mechanistic truths and physiological consequences of the time-dependent solubility of amyloid proteins. *Annu. Rev. Biochem. 66*, 385−407.

(19) Lotharius, J., and Brundin, P. (2002) Pathogenesis of Parkinson's disease: Dopamine, vesicles and alpha-synuclein. *Nat. Rev. Neurosci. 3*, 932−942.

(20) Liu, Y. C., Fallon, L., Lashuel, H. A., Liu, Z. H., and Lansbury, P. T. (2002) The UCH-L1 gene encodes two opposing enzymatic activities that affect alpha-synuclein degradation and Parkinson's disease susceptibility. *Cell 111*, 209−218.

(21) Cuervo, A. M., Stefanis, L., Fredenburg, R., Lansbury, P. T., and Sulzer, D. (2004) Impaired degradation of mutant alpha-synuclein by chaperone-mediated autophagy. *Science 305*, 1292−1295.

(22) Butterfield, S. M., and Lashuel, H. A. (2010) Amyloidogenic protein membrane interactions: Mechanistic insight from model systems. *Angew. Chem., Int. Ed. 49*, 5628−5654.

(23) Relini, A., Cavalleri, O., Rolandi, R., and Gliozzi, A. (2009) The two-fold aspect of the interplay of amyloidogenic proteins with lipid membranes. *Chem. Phys. Lipids 158*, 1−9.

(24) Linse, S., Cabaleiro-Lago, C., Xue, W., Lynch, I., Lindman, S., Thulin, E., Radford, S., and Dawson, K. (2007) Nucleation of protein fibrillation by nanoparticles. *Proc. Natl. Acad. Sci. U.S.A. 104*, 8691−8696.

(25) Necula, M., Chirita, C. N., and Kuret, J. (2003) Rapid anionic micelle-mediated alpha-synuclein fibrillization in vitro. *J. Biol. Chem. 278*, 46674−46680.

(26) Pandey, A. P., Haque, F., Rochet, J. C., and Hovis, J. S. (2009) Clustering of alpha-synuclein on supported lipid bilayers: Role of anionic lipid, protein, and divalent ion concentration. *Biophys. J. 96*, 540−551.

(27) van Rooijen, B., Claessens, M., and Subramaniam, V. (2009) Lipid bilayer disruption by oligomeric alpha-synuclein depends on

bilayer charge and accessibility of the hydrophobic core. *BBA-Biomembranes 1788*, 1271−1278.
(28) Jo, E., McLaurin, J., Yip, C., St. George-Hyslop, P., and Fraser, P. (2000) Alpha-synuclein membrane interactions and lipid specificity. *J. Biol. Chem. 275*, 34328−34334.
(29) Grey, M., Linse, S., Nilsson, H., Brundin, P., and Sparr, E. (2011) Membrane interaction of α-synuclein in different aggregation states. *J. Parkinson's Disease 1*, 359−371.
(30) Pronchik, J., He, X. L., Giurleo, J. T., and Talaga, D. S. (2010) In vitro formation of amyloid from alpha-synuclein is dominated by reactions at hydrophobic interfaces. *J. Am. Chem. Soc. 132*, 9797−9803.
(31) Breydo, L., Wu, J., and Uversky, V. (2012) Alpha-synuclein misfolding and Parkinson's disease. *Biochim. Biophys. Acta 1822*, 261−285.
(32) Ruiperez, V., Darios, F., and Davletov, B. (2010) Alpha-synuclein, lipids and Parkinson's disease. *Prog. Lipid Res. 49*, 420−428.
(33) Uversky, V. (2010) Mysterious oligomerization of the amyloidogenic proteins. *FEBS J. 277*, 2940−2953.
(34) Chiti, F., and Dobson, C. (2006) Protein misfolding, functional amyloid, and human disease. *Annu. Rev. Biochem. 75*, 333−366.
(35) Hortschansky, P., Schroeckh, V., Christopeit, T., Zandomeneghi, G., and Fandrich, M. (2005) The aggregation kinetics of Alzheimer's beta-amyloid peptide is controlled by stochastic nucleation. *Protein Sci. 14*, 1753−1759.
(36) Hellstrand, E., Boland, B., Walsh, D., and Linse, S. (2010) Amyloid beta-protein aggregation produces highly reproducible kinetic data and occurs by a two-phase process. *ACS Chem. Neurosci. 1*, 13−18.
(37) Verdes, D., Ruckstuhl, T., and Seeger, S. (2007) Parallel two-channel near- and far-field fluorescence microscopy. *J. Biomed. Opt. 12*, No. 034012.
(38) Winterflood, C. M., Ruckstuhl, T., Verdes, D., and Seeger, S. (2010) Nanometer axial resolution by three-dimensional supercritical angle fluorescence microscopy. *Phys. Rev. Lett. 105*, No. 108103.
(39) Rabe, M., Verdes, D., and Seeger, S. (2009) Surface-induced spreading phenomenon of protein clusters. *Soft Matter 5*, 1039−1047.
(40) Lee, D., Anzai, K., Hirashima, N., and Kirino, Y. (1998) Phospholipid translocation from the outer to the inner leaflet of synaptic vesicle membranes isolated from the electric organ of Japanese electric ray Narke japonica. *J. Biochem. 124*, 798−803.
(41) Schlegel, R., and Williamson, P. (2001) Phosphatidylserine, a death knell. *Cell Death Differ. 8*, 551−563.
(42) Takamori, S., Holt, M., Stenius, K., Lemke, E., Gronborg, M., Riedel, D., Urlaub, H., Schenck, S., Brugger, B., Ringler, P., Muller, S., Rammner, B., Grater, F., Hub, J., De Groot, B., Mieskes, G., Moriyama, Y., Klingauf, J., Grubmuller, H., Heuser, J., Wieland, F., and Jahn, R. (2006) Molecular anatomy of a trafficking organelle. *Cell 127*, 831−846.
(43) Domanov, Y., and Kinnunen, P. (2008) Islet amyloid polypeptide forms rigid lipid-protein amyloid fibrils on supported phospholipid bilayers. *J. Mol. Biol. 376*, 42−54.
(44) Reynolds, N., Soragni, A., Rabe, M., Verdes, D., Liverani, E., Handschin, S., Riek, R., and Seeger, S. (2011) Mechanism of membrane interaction and disruption by alpha-synuclein. *J. Am. Chem. Soc. 133*, 19366−19375.
(45) Andersen, C. B., Yagi, H., Manno, M., Martorana, V., Ban, T., Christiansen, G., Otzen, D. E., Goto, Y., and Rischel, C. (2009) Branching in amyloid fibril growth. *Biophys. J. 96*, 1529−1536.
(46) Yagi, H., Ban, T., Morigaki, K., Naiki, H., and Goto, Y. (2007) Visualization and classification of amyloid beta supramolecular assemblies. *Biochemistry 46*, 15009−15017.
(47) Giehm, L., Lorenzen, N., and Otzen, D. (2011) Assays for alpha-synuclein aggregation. *Methods 53*, 295−305.
(48) Giehm, L., Svergun, D., Otzen, D., and Vestergaard, B. (2011) Low-resolution structure of a vesicle disrupting alpha-synuclein oligomer that accumulates during fibrillation. *Proc. Natl. Acad. Sci. U.S.A. 108*, 3246−3251.
(49) Pandey, A., Haque, F., Rochet, J., and Hovis, J. (2011) Alpha-synuclein-induced tubule formation in lipid bilayers. *J. Phys. Chem. B 115*, 5886−5893.
(50) Li, J., Uversky, V. N., and Fink, A. L. (2001) Effect of familial Parkinson's disease point mutations A30P and A53T on the structural properties, aggregation, and fibrillation of human alpha-synuclein. *Biochemistry 40*, 11604−11613.
(51) Conway, K. A., Lee, S. J., Rochet, J. C., Ding, T. T., Williamson, R. E., and Lansbury, P. T. (2000) Acceleration of oligomerization, not fibrillization, is a shared property of both alpha-synuclein mutations linked to early-onset Parkinson's disease: Implications for pathogenesis and therapy. *Proc. Natl. Acad. Sci. U.S.A. 97*, 571−576.
(52) Winner, B., Jappelli, R., Maji, S., Desplats, P., Boyer, L., Aigner, S., Hetzer, C., Loher, T., Vilar, M., Campionic, S., Tzitzilonis, C., Soragni, A., Jessberger, S., Mira, H., Consiglio, A., Pham, E., Masliah, E., Gage, F., and Riek, R. (2011) In vivo demonstration that alpha-synuclein oligomers are toxic. *Proc. Natl. Acad. Sci. U.S.A. 108*, 4194−4199.
(53) Rabe, M., Verdes, D., Rankl, M., Artus, G. R. J., and Seeger, S. (2007) A comprehensive study of concepts and phenomena of the nonspecific adsorption of beta-lactoglobulin. *ChemPhysChem 8*, 862−872.
(54) Rabe, M., Verdes, D., Zimmermann, J., and Seeger, S. (2008) Surface organization and cooperativity during nonspecific protein adsorption events. *J. Phys. Chem. B 112*, 13971−13980.
(55) Levine, H. (1993) Thioflavine-T interaction with synthetic Alzheimers-disease beta-amyloid peptides - detection of amyloid aggregation in solution. *Protein Sci. 2*, 404−410.
(56) Haque, F., Pandey, A. P., Cambrea, L. R., Rochet, J. C., and Hovis, J. S. (2010) Adsorption of alpha-synuclein on lipid bilayers: Modulating the structure and stability of protein assemblies. *J. Phys. Chem. B 114*, 4070−4081.
(57) Kuznetsova, I., Sulatskaya, A., Uversky, V., and Turoverov, K. (2012) Analyzing thioflavin T binding to amyloid fibrils by an equilibrium microdialysis-based technique. *PLOS One 7*, No. e30724.
(58) Yoshimura, Y., Lin, Y., Yagi, H., Lee, Y.-H., Kitayama, H., Sakurai, K., So, M., Ogi, H., Naiki, H., and Goto, Y. (2012) Distinguishing crystal-like amyloid fibrils and glass-like amaorphous aggregates from their kinetics of formation. *Proc. Natl. Acad. Sci. U.S.A. 109*, 14446−14451.
(59) Kayed, R., Head, E., Sarsoza, F., Saing, T., Cotman, C., Necula, M., Margol, L., Wu, J., Breydo, L., Thompson, J., Rasool, S., Gurlo, T., Butler, P., and Glabe, C. (2007) Fibril specific, conformation dependent antibodies recognize a generic epitope common to amyloid fibrils and fibrillar oligomers that is absent in prefibrillar oligomers. *Mol. Neurodegener. 2*, 1−11.
(60) Hoyer, W., Cherny, D., Subramaniam, V., and Jovin, T. (2004) Rapid self-assembly of alpha-synuclein observed by in situ atomic force microscopy. *J. Mol. Biol. 340*, 127−139.
(61) Giehm, L., Oliveira, C. L. P., Christiansen, G., Pedersen, J. S., and Otzen, D. E. (2010) SDS-induced fibrillation of alpha-synuclein: An alternative fibrillation pathway. *J. Mol. Biol. 401*, 115−133.
(62) Zhu, M., Souillac, P. O., Ionescu-Zanetti, C., Carter, S. A., and Fink, A. L. (2002) Surface-catalyzed amyloid fibril formation. *J. Biol. Chem. 277*, 50914−50922.
(63) Sluzky, V., Tamada, J., Klibanov, A., and Langer, R. (1991) Kinetics of insulin aggregation in aqueous-solutions upon agitation in the presence of hydrophobic surfaces. *Proc. Natl. Acad. Sci. U.S.A. 88*, 9377−9381.
(64) Bourgault, S., Solomon, J., Reixach, N., and Kelly, J. (2011) Sulfated glycosaminoglycans accelerate transthyretin amyloidogenesis by quaternary structural conversion. *Biochemistry 50*, 1001−1015.
(65) Solomon, J., Bourgault, S., Powers, E., and Kelly, J. (2011) Heparin binds 8 kDa gelsolin cross-beta-sheet oligomers and accelerates amyloidogenesis by hastening fibril extension. *Biochemistry 50*, 2486−2498.
(66) Roberti, M. J., Bertoncini, C. W., Klement, R., Jares-Erijman, E. A., and Jovin, T. M. (2007) Fluorescence imaging of amyloid

formation in living cells by a functional, tetracysteine-tagged alpha-synuclein. *Nat. Methods 4*, 345−351.
(67) Liu, R. C., Hu, D. H., Tan, X., and Lu, H. P. (2006) Revealing two-state protein−protein interactions of calmodulin by single-molecule spectroscopy. *J. Am. Chem. Soc. 128*, 10034−10042.
(68) Carson, F. L. (1997) *Histotechnology: A Self-Instructional Text*, 2nd ed., pp 125−129, American Society of Clinical Pathologists, Chicago.